Palaeogeography, Palaeoclimatology, Palaeoecology, 71 (1989): 119–136
Elsevier Science Publishers B.V., Amsterdam — Printed in The Netherlands

METHANE-DERIVED CO_2 IN PORE FLUIDS EXPELLED FROM THE OREGON SUBDUCTION ZONE

E. SUESS[1,3] and M. J. WHITICAR[2]

[1]*College of Oceanography, Oregon State University, Corvallis, OR 97331 (U.S.A.)*
[2]*Bundesanstalt für Geowissenschaften und Rohstoffe, 3000 Hannover 51 (F.R.G.)*

(Received January 9, 1988; revised and accepted March 22, 1988)

Abstract

Suess, E. and Whiticar, M. J., 1989. Methane-derived CO_2 in pore fluids expelled from the Oregon subduction zone. Palaeogeogr., Palaeoclimatol., Palaeoecol., 71: 119–136.

Pore fluids extracted from near-surface sediments of the deformation front along the Oregon subduction zone have, in general, the dissolved nutrient pattern characteristic of bacterial sulfate reduction. However, in certain locations there are peculiar ammonium distributions and anomalously ^{13}C-depleted dissolved ΣCO_2. These carbon isotope and nutrient patterns are attributed to the concurrent microbially-mediated oxidation of sedimentary organic matter (POC) and methane (CH_4) originating from depth. In contrast to the oxidation of sedimentary organic matter in the sulfate zone, utilization of methane as the carbon source by sulfate-reducing bacteria would generate only half as much total carbon dioxide for each mole of sulfate consumed and would not generate any dissolved ammonium. The isotopically light ΣCO_2 released from methane oxidation depletes the total metabolic carbon dioxide pool. Therefore, NH_4^+, ΣCO_2 and $\delta^{13}C$ of interstitial carbon dioxide in these pore fluids distinctly reflect the combined contributions of each of the two carbon substrates undergoing mineralization; i.e. methane and sedimentary organic matter. By appropriately partitioning the nutrient and substrate relationships, we calculate that in the area of the marginal ridge of the Oregon subduction zone as much as 30% of the ΣCO_2 in pore fluids may result from methane oxidation. The calculation also predicts that the carbon isotope signature of the carbon dioxide derived from methane is between −35‰ and −63‰ PDB. Such an isotopically light gas generated from within the accretionary complex could be the residue of a biogenic methane pool. Fluid advection is required to carry such methane from depth to the present near-surface sediments. This mechanism is consistent with large-scale, tectonically-induced fluid transport envisioned for accreted sediments of the world's convergent plate boundaries.

Introduction

The deep-sea submersible *Alvin* has provided structural and stratigraphic data on the framework of plate subduction along the northeast Pacific convergence zone and has visited deep sites of fluid venting in the underthrust tectonic setting of the Oregon margin. Communities of clams and tube worms, authigenic carbonate minerals, methane-enriched bottom waters, and biological tissues with extreme ^{12}C isotope enrichment were collected at this accretionary complex where the Juan de Fuca oceanic plate plunges beneath the North American continental plate (Suess et al., 1985; Kulm et al., 1986; Schroeder et al., 1987). Equally exciting new information on the chemistry of fluids and vent organisms was gathered by the submersible *Nautile* from the subducting plate boundaries of the northwest Pacific (Le Pichon et al., 1987; Boulegue et al., 1987). The drilling vessel *Joides Resolution*

[3]Present address: GEOMAR Research Center, Wischhofstr. 1-3, 2300 Kiel 14 (F.R.G.).

0031-0182/89/$03.50

recently penetrated the décollement between the converging Caribbean and Atlantic plates near the Barbados deformation front and also found anomalous pore water ion and methane concentrations, as evidence for active fluid movement along fault planes (Moore et al., 1986). It appears that in modern and ancient accreted deposits methane and, perhaps, higher hydrocarbons dissolved in venting pore fluids play a unique role in providing energy and carbon for the benthic communities of large vent organisms and for the lithification of accretionary deposits by carbonate cement (Han and Suess, this issue). We have earlier hypothesized, inferred from pore fluid chemical anomalies, that such a methane-based biogeochemical system operates at the Oregon subduction zone (Suess et al., 1985; Kulm et al., 1986). We will now substantiate and extend this reaction mechanism by presenting stable carbon isotope data of ΣCO_2 from pore fluids of the deformation front. These fluids contain dissolved metabolic carbon dioxide which is depleted with ^{13}C beyond what is expected from mineralization of normal sedimentary organic matter. The pore water data are explained by a mixing model whereby concurrent microbial oxidation of sedimentary organic matter (POC) and the chemically more reduced methane carbon substrate (CH_4) account for the observed nutrient and isotope patterns. Moreover, the isotope signature of the postulated methane-derived ΣCO_2 is consistent with that of methane-derived dolomite and magnesian calcite cements of the Oregon accretionary complex. The $\delta^{13}C$ characteristics of the diagenetic carbonates and the metabolic carbon dioxide range from -35 to -66‰ PDB and indicate a residual biogenic source for the methane.

Coring sites at the Oregon subduction zone

The style of sediment accretion along portions of the Oregon subduction zone includes stacked sequences of landward dipping and seaward dipping packages of hemipelagic sediments of the Astoria fan separated by thrust planes (Kulm and Fowler, 1974). The morpho-

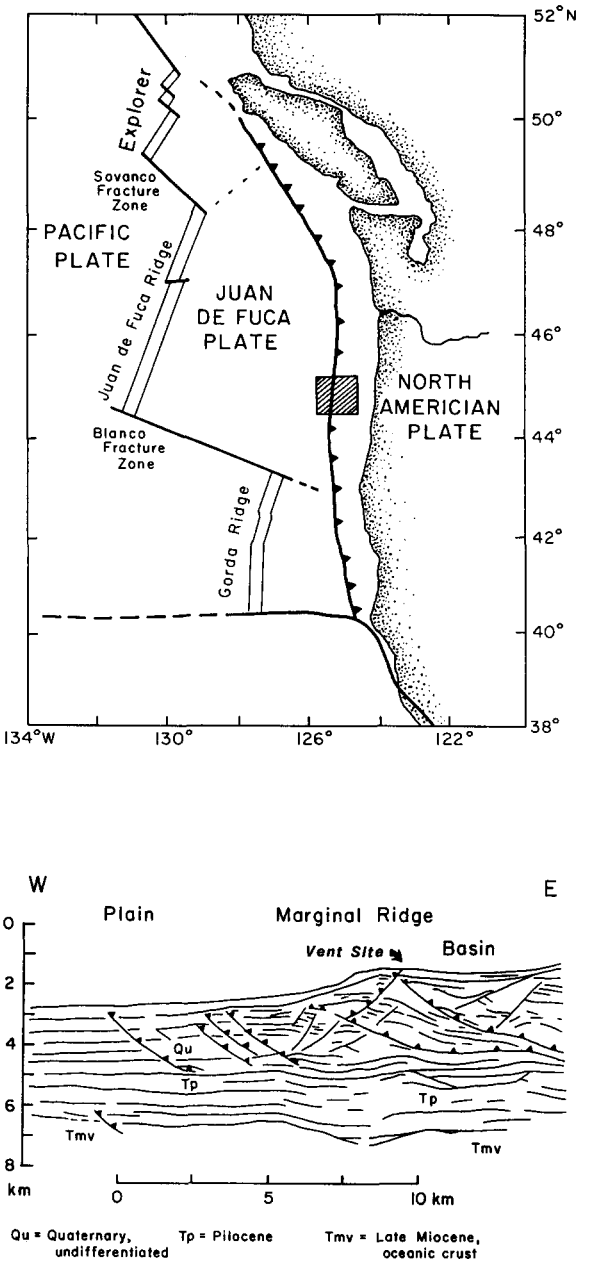

Fig.1. (Top). Northeastern Pacific plates; the Juan de Fuca plate is subducted as it converges with the North American plate. An accretionary complex forms by off-scraping sediments from the oceanic plate. In the area of investigation (box) the tectonic style of subduction is by underthrusting. (Bottom), The convergence-induced lateral stress causes large-scale dewatering of the accretionary complex along the main décollement surface and numerous landward dipping fault planes. An area of extensive venting of fluids is located just off the ridge crest (Vent Site). The tectonic elements of convergence are: undeformed abyssal plain, marginal ridge, and ponded basin.

logical expression of the accreted stacks is a series of north–south trending thrust ridges with intervening basins of ponded sediments. In the study area (Fig.1A and B) the initial deformation front is a seaward-facing scarp at the toe of the continental slope that rises 4–6 m above the abyssal plain. A second scarp, exposed a few hundred meters landward, apparently is the outcrop of the décollement surface which separates the deformed off-scraped deposits of the thrust ridge from the more gently dipping strata which are being subducted with the converging oceanic plate. A transect of gravity cores and pore water profiles was obtained across these tectonic elements of the Oregon subduction zone (Fig.2; Table I). Two cores [8408-04 and 8408-11] were raised from the gently dipping strata between the escarpments, which showed not evidence of deformation. The main underthrust ridge rises steeply, more than 800 m, above the abyssal plain. The seaward face of this ridge is cut by

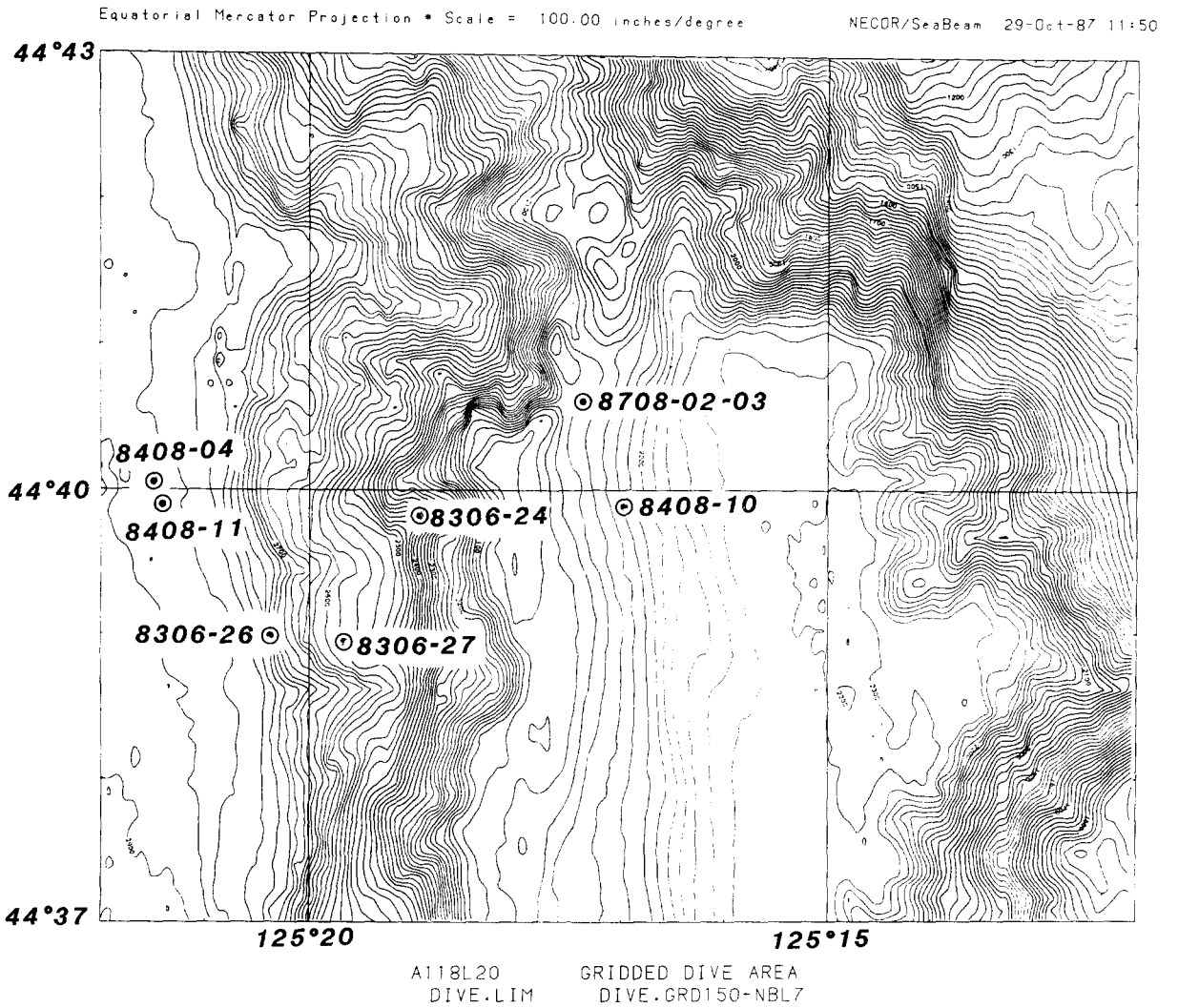

Fig.2. SeaBeam bathymetry (20 m depth contours) and core locations in the underthrust tectonic setting off Oregon. Cores 8408-04 and 8408-11, at the toe of the continental slope, are seaward of the deformation front. Cores 8306-26, 8306-27 and 8306-24 are on the seaward face of the underthrust ridge. Cores 8708-02 and 8708-03 are located at the vent site, and Core 8408-10 at the western edge of the ponded sediment basin.

TABLE I

Station locations and water depths of coring transect across deformation front of the Oregon subduction zone

Station	Latitude (°N)	Longitude (°W)	Water depth (m)
8306-24	44°39.78′	125°19.07′	2420
8306-26	44°39.00′	125°20.50′	2795
8306-27	44°39.00′	125°19.66′	2623
8408-04	44°40.00′	125°21.60′	2860
8408-10	44°40.00′	125°17.10′	2180
8408-11	44°39.90′	125°21.50′	2846
8708-02	44°40.55′	125°17.43′	2040
8708-03	44°40.55′	125°17.43′	2040

canyons and exposes mainly rocks but in part is covered by patches of sediment which accumulate on morphological ledges. Three cores [8306-24, 8306-26, and 8306-27] were collected from these patches on the seaward face of the underthrust ridge. Along the landward flank of the ridge, just off its crest, the benthic communities of tube worms and giant clams were observed during *Alvin* dives (Suess et al., 1985; 1987a). Two cores (8708-02 and 8708-03) were taken from the sediment patch surrounding the vent site; core 8708-03 was collected within 10 m of the giant white clam and tube worm communities. Finally, one core (8408-10) was taken from the westernmost part of the sediment pond near the unconformity with the underthrust ridge, about 200 m distant from the vent site.

Sampling and analyses

Interstitial waters were extracted from sediments of these eight stations by pressure filtration at the temperature of the bottom water close to 2°C with a technique initially described by Hartmann et al. (1973). For the highly compacted sediments at the underthrust ridge a hydraulic press and sample cell was used similar to the system adopted by the Ocean Drilling Program (Manheim and Sayles, 1974). Total dissolved carbon dioxide (ΣCO_2) was determined by on-line gas chromatography and quantified by thermal conductivity after acidification and He-stripping of the interstitial waters. Dissolved chloride was determined by the standard Mohr-titration, sulfate gravimetrically as $BaSO_4$, ammonium by standard methods for nutrient analyses in seawater (Grasshoff, 1976) and calcium and magnesium by flame atomic absorption spectrometry. The results are reported in units of g/kg for chlorinity and mmol/L (mM), mg/L or μmol/L (μM) for the other dissolved species along with precision estimates (Table II). Samples for stable carbon isotope measurements of ΣCO_2 and deuterium/hydrogen ratios of water were drawn into Vacutainers® and treated with mercuric chloride. The dissolved ΣCO_2 was prepared for $^{13}C/^{12}C$ measurement by the standard method of acidification and collection at 25°C. The interstitial H_2O was reduced to hydrogen for D/H measurement by freezing the H_2O over onto zinc-filled 6 mm glass tubes which were evacuated, sealed and heated to 460°C (Coleman et al., 1982). All isotope mass ratios were measured using a Finnegan MAT 251 mass spectrometer. The results are reported in the usual delta notation (Table III):

$$\delta R = \left[\frac{R_a/R_b \text{ sample} - R_a/R_b \text{ standard}}{R_a/R_b \text{ standard}}\right] 1000 \quad (1)$$

where R_a/R_b are the $^{13}C/^{12}C$ and D/H ratios relative to the PDB standard for carbon and the SMOW-(H_2O) standard for hydrogen.

The organic-carbon-to-organic-nitrogen ratio ($C/N_{\text{by atoms}}$) of sedimentary organic matter of the Oregon margin sediments was needed to evaluate the C/N rgeneration ratio of POC during microbial sulfate reduction. For this purpose organic carbon and carbonate carbon contents were determined on five of the cores using the H_3PO_4/dichromate-LECO technique described by Weliky et al. (1983). Basically, carbonate–carbon is measured as the CO_2 liberated during treatment of the sediment with phosphoric acid, and organic carbon is measured as the CO_2 evolved during subsequent oxidation of the remaining sediment and phosphoric acid mixture with dichromate. The

TABLE II

Pore water data from eight gravity cores across the Oregon margin deformation front; the accuracy of chlorinities marked by (*) is affected by dilution and/or loss by evaporation, therefore the Na-contents of these samples were used to calculate the Ca^{2+} and Mg^{2+} decrease

Core station	Depth interval (cm)	NH_4 (μM)	ΣCO_2 (mM)	SO_4 (mM)	Ca (mg/L)	Mg (mg/L)	Cl (g/kg)
8408-04	20–23	192	4.47	27.16	432	1310	19.34
	55–58	501	7.91	24.94	417	1290	19.15
	90–93	689	9.88	23.14	400	1290	18.84*
	125–128	1022	13.84	20.84	376	1280	18.74*
	160–163	1154	15.83	19.45	356	1250	18.93*
	195–198	1340	18.35	17.67	323	1250	19.06
8404-10	0–5	26	2.80	27.88	428	1310	19.10
	20–25	150	3.93	27.08	425	1290	19.42
	50–55	296	5.59	26.02	401	1250	19.39
	215–220	1508	20.53	11.46	172	1201	20.69*
8408-11	0–5	33	3.18	28.17	418	1260	18.95
	20–25	172	4.36	27.19	410	1290	19.24
	65–70	699	10.42	22.32	379	1270	19.10
	120–125	955	12.78	20.09	342	1250	19.35
8708-02	30–40	33	3.12	27.71	419	1301	19.22
	60–70	38	3.17	27.62	417	1293	19.29
	92–98	85	3.27	27.28	409	1284	19.29
	115–120	124	3.29	26.70	405	1274	19.37
	140–147	256	5.54	24.75	380	1259	19.26
	166–172	441	9.05	19.19	333	1247	19.47
	195–200	722	11.66	14.20	270	1177	19.20
	215–220	711	14.92	11.36	249	1196	19.41
8708-03	7–12	42	3.33	27.24	419	1313	19.46
	20–26	87	3.56	26.59	416	1281	19.31
	32–39	126	4.16	25.87	402	1286	18.94
	56–61	197	4.13	24.44	391	1272	19.05
	82–87	300	5.25	23.36	361	1242	19.14
	112–117	463	6.88	18.93	303	1191	19.22
8306-24	5–10	71.0	3.10	26.86	410	1284	19.10
	25–30	230.0	5.20	25.39	406	1309	19.28
	60–65	539.0	8.60	22.04	384	1249	19.09
	85–90	740.0	10.60	19.97	338	1184	18.60*
	125–130	758.0	12.80	15.42	313	1177	19.45
	160–165	1114.0	15.40	12.72	286	1149	19.45
	175–180	1039.0	15.30	11.54	275	1134	19.45
8306-26	5–10	126.0	4.00	26.94	415	1294	19.74
	25–30	178.0	4.90	25.84	412	1293	19.41
	45–50	389.0	7.80	24.52	397	1287	18.92*
	70–75	824.0	13.00	22.71	377	1270	19.54
	92–98	923.0	15.30	21.01	358	1285	19.17
	100–105	1037.0	16.80	20.08	335	1282	19.52
	105–110	1013.0	17.00	19.57	334	1292	19.67
	110–115	1002.0	18.10	19.25	338	1276	19.45
8306-27	20–25	162.0	3.75	26.09	403	1288	19.48
	50–55	261.0	4.83	24.68	395	1289	19.41
	70–75	339.0	5.78	23.91	382	1331	19.63
	90–95	402.0	6.63	22.84	361	1278	19.49
	105–110	437.0	7.19	22.62	353	1254	19.34
	130–135	516.0	8.45	21.53	337	1269	18.36
	145–150	633.0	9.45	20.59	320	1231	19.16

TABLE II (*continued*)

		Standard seawater
Cl^-	Titration with $AgNO_3$	0.06% or 0.01‰
SO_4	Gravimetry	<1% or 0.15 mM
Mg	Flame AAS	1% or 0.5 mM
Ca	Flame AAS	1% or 0.1 mM
ΣCO_2	GC-Therm. Cond	2% or 0.05 mM
NH_4	Colorimetry	3% or 0.5 μM
PO_4	Colorimetry	0.5% or 0.1 μM

Propagation of analytical uncertainties cause the ΣCO_2 estimates in Figs.4A–D and 5A–D to be precise by ±12%; i.e. ±0.3 mM for estimates in the range of ΣCO_2 of seawater and ±1.5 mM for estimates >10.0 mM.

TABLE III

Stable carbon isotopes of dissolved ΣCO_2 and deuterium/hydrogen ratios of H_2O from selected pore water samples of the Oregon subduction zone. Note: extreme ^{13}C-depletion of ΣCO_2 in deep pore waters of Stations 8306-24, 8306-27 and 8708-02

Core no.	Depth (cm)	$\delta^{13}CO_{2(meas)}$ (‰ PDB)	ΣCO_2 (mM)	$\delta D_{(water)}$ (‰ SMOW)
8306-24	25–30	−15.2	5.2	1.2
	85–90	−23.1	10.6	2.6
	160–165	−26.3	15.4	0.7
8306-26	25–30	−13.1	4.9	1.5
	70–75	−18.5	13.8	—
	100–105	−18.4	16.8	−1.4
8306-27	20–25	−13.3	3.75	0.5
	50–55	−19.2	4.83	1.3
	70–75	−20.7	5.78	−1.2
	90–95	−21.3	6.63	0.2
	105–110	−23.4	7.19	0.3
	130–135	−24.3	8.45	—
	145–150	−24.7	9.45	−0.2
8408-04	125–130	−18.3	13.84	0.1
	160–163	−16.6	15.83	0.1
8708-02	60–70	−13.5	3.17	—
	115–120	−23.9	3.29	—
	215–220	−34.8	14.92	—

CO_2 is detected by a thermal conductivity detector. Total nitrogen was determined using the micro-Kjeldahl digestion method described by Bremner (1960). Inorganic fixed ammonium-nitrogen was determined by the method of Silva and Bremner (1966). In this procedure, the organically-bound nitrogen is first removed with potassium hypobromite. The residue is then treated with hydrofluoric acid to destroy the silicate lattice structure of clay minerals. The solution is made basic with KOH and the nitrogen is distilled as NH_4 and detected as in the micro-Kjeldahl technique. Organic nitrogen is calculated as the difference between the

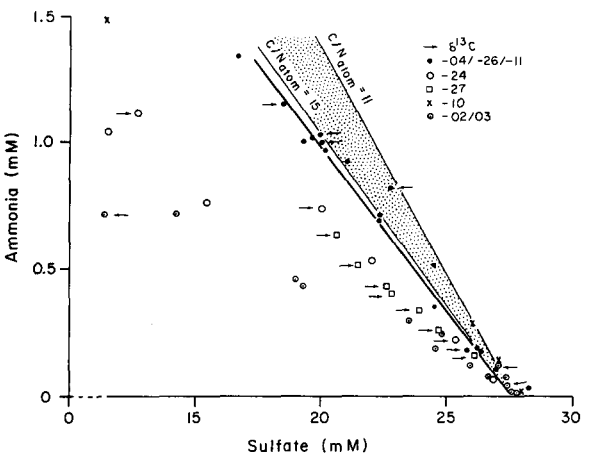

Fig.3. Dissolved ammonium and sulfate concentrations in the pore waters show two groupings: the solid symbols which denote stations with ammonium generated as expected from microbial sulfate reduction of normal sedimentary organic matter (POC) and the open symbols which denote stations with strong negative ammonium anomalies compared to the observed sulfate reduction. This deficit reflects the lack of ammonium released from the anaerobic oxidation of methane (CH_4). The regression line indicates the regeneration ratio $NH_4^+ : -SO_4^{2-} = 7 : -53$ used in Eq.(2). The stippled area covers the regeneration ratios $NH_4^+ : SO_4^{2-}$ between $7.07 : -53$ (C/N = 15) and $9.64 : -53$ (C/N = 11) as estimated from the organic carbon and organic nitrogen analyses of the Oregon margin cores. The arrows indicate samples from which $\delta^{13}CO_2$ data were obtained (for results see Table III).

total nitrogen and fixed nitrogen. The results of the C/N ratios are incorporated into Fig.3, the data, however, are reported elsewhere (Han, 1987).

Pore water chemistry: substrates for metabolic CO_2 production

Pore waters from the sediments of the marginal ridge and the undeformed toe of the continental slope show patterns of dissolved constituents characteristic of mineralization of organic matter by microbial sulfate reduction, i.e., an increase of ΣCO_2, and NH_4^+ and a corresponding decrease of dissolved SO_4^{2-} with depth in core (Fig.3; Table II). This is expected for hemipelagic environments of the type represented by the Astoria fan deposits (Waterman et al., 1972; Hartmann et al., 1973; Claypool, 1974; Suess, 1976). Also, as in similar continental margin settings, the interstitial dissolved Ca^{2+} and Mg^{2+} contents decrease due to formation of diagenetic carbonate minerals at greater depth in the sediment. Dolomite, high- and low-Mg calcites, and aragonite are ubiquitous in the Oregon margin sediments (Russell et al., 1967; Scamman, 1981; Ritger et al., 1987; Han and Suess, this issue).

We assume for this discussion that along the Oregon subduction zone all of the Ca^{2+} and Mg^{2+} decrease observed in pore waters is consumed by diagenetic carbonate mineral formation. This assumption is justified and discussed in detail in this volume by Han and Suess, and elsewhere (Han, 1987). It most likely overestimates the ΣCO_2 removal from pore fluids, because it does not consider alteration of volcano-clastics and terrigenous aluminosilicates. In many cases, however, there is a 1:1 molar decrease of both Ca^{2+} and Mg^{2+} as would be expected from dolomite formation. Since this diagenetic mineral is common in the carbonate crusts, concretions, chimneys and cements of the lithified accretionary deposits (Ritger et al., 1987), we think that the above assumption is well-justified. The simple stoichiometric nutrient-regeneration-mineral-precipitation may then be approximated by the reaction:

$$2[(CH_2O)(NH_3)x] + SO_4^{2-} + Ca^{2+} + Mg^{2+} \rightarrow$$
$$[CaMg(CO_3)_2] + xNH_4^+ + H_2S \quad (2)$$

Hereby x denotes the inverse of the carbon-to-nitrogen regeneration ratio. Hydrogen sulfide is not considered because it takes part in a series of reactions involving more complex solid phases whose stoichiometry cannot be as readily approximated as that of dolomite or calcites (Berner, 1977, 1980). Ammonium, except for ion-exchange, accumulates in the anoxic pore fluids and is a sensitive indicator for the oxidation of sedimentary organic matter (POC) by microbial sulfate reducers.

At certain localities across the main underthrust ridge of the Oregon subduction zone, the regenerated nutrient pattern is anomalously depleted in NH_4^+ and ΣCO_2 relative to the observed interstitial SO_4^{2-} removal. Only the NH_4^+-distribution is shown in Fig.3; the open symbols are for samples from the deformed sediments, the closed symbols denote the tectonically undeformed sediment samples from the toe of the continental slope. The NH_4^+-deficit seen in the pore fluids of the deformed sediments is larger than that of the most nitrogen-depleted organic matter of the Oregon margin sediments [lower limit C/N (by atoms) = 15; Fig.3]. The upper limit in this figure shows a regenerative ratio of $-SO_4^{2-}:NH_4^+ = -53:9.64$ which corresponds to the mean ratio of C-organic/N-organic$_{(\text{by atoms})} = 11$ in five of the sediment cores analyzed. It is commonly assumed that uptake of ammonium by ion-exchange significantly reduces the ratio between SO_4^{2-}-consumption and NH_4^+-release (Rosenfeld, 1981; Boatman and Murray, 1982). This process is likely the reason for the overall deviation between the C/N-ratio of POC in the sediments and that actually observed in the pore water; i.e. the discrepancy in Fig.3 between the trend followed by the solid symbols and that covered by the stippled area.

Eighteen samples out of a total of 50 were selected for $\delta^{13}\Sigma CO_2$ analyses. These samples

are indicated by horizontal arrows in Fig.3 and the results listed in Table III. The ΣCO_2-depletion in the samples relative to sulfate reduction not illustrated here, remains significant even after adjustment for removal by carbonate formation based on Ca^{2+}- and Mg^{2+}-losses. We attribute the anomalies in NH_4^+ and ΣCO_2 to the oxidation of methane because in utilizing such a carbon substrate, microbial sulfate reducers generate only half as much metabolic ΣCO_2 as they generate from utilizing normal sedimentary organic matter (POC). Methane oxidation generates no NH_4^+ at all. Anaerobic methane oxidation is by now well-established as an early diagenetic process in anoxic hemipelagic sediments (Devol, 1983; Iversen and Jørgensen, 1985; Whiticar and Faber, 1986). Aerobic methane consumption has been shown by mussels at seep communities (Childress et al., 1986). The different ΣCO_2-regeneration and SO_4^{2-}-reduction ratios are evident from the following comparison:

Methane oxidation:

$$CH_4 + SO_4^{2-} = \Sigma CO_2 + 2H_2O + S^{2-} \quad (3)$$

$$\Sigma CO_2 : -SO_4^{2-} = 1:1$$

Sedimentary organic matter oxidation:

$$2[(CH_2O)(NH_4)x] + SO_4^{2-} =$$

$$2\Sigma CO_2 + 2H_2O + 2xNH_4^+ + S^{2-}$$

$$\Sigma CO_2 : -SO_4^{2-} = 2:1$$

Therefore, the NH_4^+ and ΣCO_2-anomalies in pore fluids from the localities at the underthrust ridge may reflect the combined contributions of each of the two substrates — POC and CH_4 — undergoing concurrent mineralization. The contributions can be calculated from the NH_4^+-anomaly in the pore fluids, the dissolved SO_4^{2-}-change, the Ca^{2+} and Mg^{2+} losses, and the organic-carbon-to-organic-nitrogen ratios of the POC substrate as follows:

$$\Sigma CO_2 = k + \Delta NH_4^+ \times C/N + \quad (4)$$

$$(\Delta SO_4^{2-} - \Delta NH_4^+ \times 1/2 C/N) -$$

$$(\Delta Ca^{2+} + \Delta Mg^{2+})$$

Hereby is ΣCO_2 the predicted total dissolved carbon dioxide content in any pore water sample. This prediction assumes equal diffusivities for all dissolved components. The constant k denotes the quantity of ΣCO_2 buried with the oceanic bottom water; usually an amount of ~ 2.6 mM. The term, $\Delta NH_4 \times C/N$, quantifies the metabolic ΣCO_2 contributed by the oxidation of POC; hereby C/N is the regeneration ratio of the POC-substrate; i.e. $C/N_{\text{by atoms}} = 15$. The next term, $\Delta SO_4^{2-} - \Delta NH_4^+ \times 1/2 C/N$, is the amount of metabolic ΣCO_2 derived from CH_4. The expression, $\Delta NH_4^+ \times 1/2 C/N$, is equivalent to the amount of SO_4^{2-} reduced during POC oxidation and the factor 1/2 scales C/N to SO_4^{2-}/NH_4^+ according to the Redfield stoichiometry. The difference between the total change in sulfate and that consumed by POC is the SO_4^{2-} consumed in CH_4-oxidation, because Eq.(3) specifies that $\Delta SO_4^{2-} : \Delta \Sigma CO_{2\,\text{methane}} = 1:1$. The last term, $\Delta Ca^{2+} + \Delta Mg^{2+}$, is a simple measure for the amount of ΣCO_2 removed by carbonate mineral formation, as discussed previously.

The results of partitioning of metabolic ΣCO_2 according to Eq.(4) are shown in Figs.4 and 5. Core 8708-02 (Fig.4A) is discussed in greater detail because it shows all the important features. The discussion applies, correspondingly, to the other cores. In Core 8708-02, at about 130 cm below the seafloor, a discontinuity separates the onlapping ponded sediments above from the deformed ridge sediments below. In the deeper sediments the NH_4^+-anomaly is significant and used to predict the ΣCO_2 contributed from CH_4-oxidation (heavy solid line). The predicted ΣCO_2 and measured values (solid symbols connected by dashed line) agree very well. The gross ΣCO_2 produced prior to carbonate mineral precipitation is shown by the dotted line. The precipitation of diagenetic carbonates, from the sum of the Ca^{2+} and Mg^{2+} losses, reduces the gross ΣCO_2 prediction to the level shown by the heavy solid line without symbols. The open symbols show the predicted ΣCO_2 contribution from CH_4-oxidation according to the term $[\Delta SO^{2-} - \Delta NH + 1/2 C/N]$ from Eq.(4). This pre-

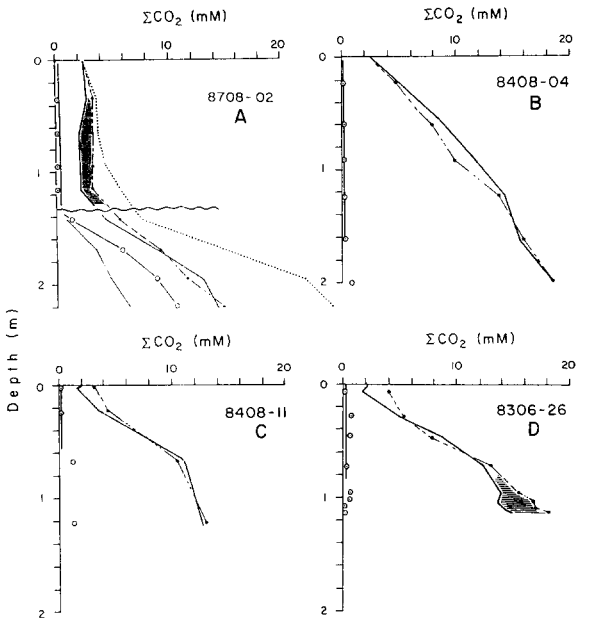

Fig.4. Predicted partitioning for ΣCO_2 according to Eq.(4) in pore waters of cores 8708-02 (A), 8408-04 (B), 8408-11 (C), and 8306-26 (D): The dotted line (Fig.4A only) shows the gross ΣCO_2 resulting from seawater burial, POC- and CH_4-oxidation prior to Ca–Mg-carbonate precipitation. The heavy solid lines without symbols show the predicted ΣCO_2-content after correction for carbonate mineral precipitation. The dashed lines with closed symbols indicate the measured ΣCO_2-contents. The contributions of CH_4-derived ΣCO_2 are shown by the open symbols, prior to carbonate precipitation, and by the thin solid lines after correction for carbonate precipitation. The horizontal pattern denotes a discrepancy between predicted and measured ΣCO_2 which is greater than expected from the uncertainty of the analytical data (see Table II).

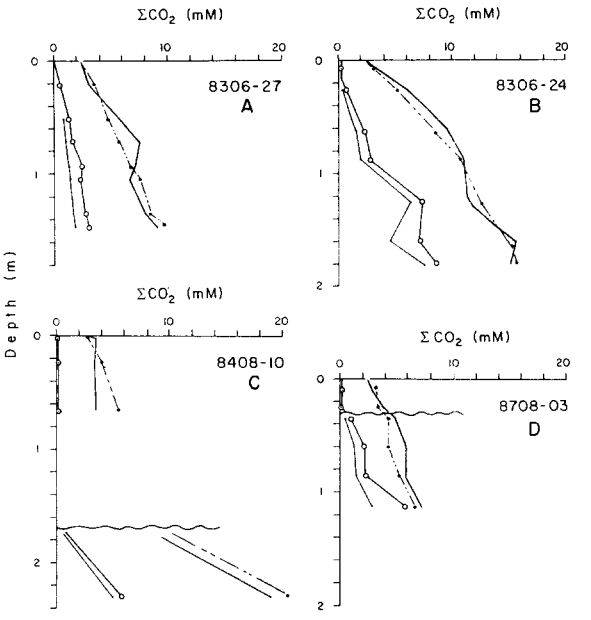

Fig.5. Predicted partitioning for ΣCO_2 according to Eq.(4) in pore waters of cores 8306-27 (A), 8306-24 (B), 8408-10 (C), and 8708-03 (D). The measured, predicted, and CH_4-derived ΣCO_2 contents are shown by the same symbols as in Fig.4; the gross ΣCO_2-content prior to carbonate mineral precipitation is omitted.

diction does not take into account the carbonate mineral precipitation and therefore should be evaluated vis-a-vis the gross ΣCO_2 production. Finally, the CH_4-derived ΣCO_2, corrected for carbonate mineral precipitation, is shown by the trend of the small solid symbols connected by the thin solid line. In the ponded sediment section of Core 8708-02, the measured ΣCO_2 contents change little with depth as do the predicted values, although the two disagree by more than the estimated uncertainties (horizontally shaded area). Tentatively, we think that this may reflect a partial oxidation of methane by dissolved oxygen rather than by sulfate and thus the ammonium anomaly would not accurately predict the amount of CH_4-derived ΣCO_2. The upper sediment is coarse-grained and the site of active fluid venting and aerobic methane oxidation a likely process.

In the remaining seven cores (Figs.4B–D and 6A–D) the measured and predicted ΣCO_2 are shown and, when applicable, the total methane-derived ΣCO_2 (open symbols) and the precipitation-corrected methane-derived ΣCO_2 contents (small solid symbols connected by thin solid lines). For simplicity, the gross ΣCO_2, generated prior to carbonate precipitation, is omitted.

Along the transect, from the deformation front to the sediment pond, the agreement between predicted and measured ΣCO_2 is quite good. Three distinct groupings are evident: First, Cores 8408-04, 8306-26, and 8408-11 contain no to insignificantly small contributions of methane-derived ΣCO_2 in their pore fluids. A

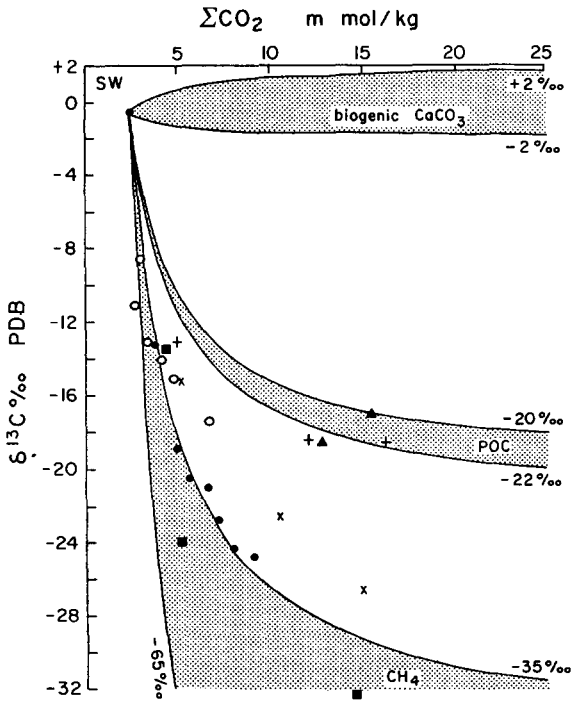

Fig.6. Total CO_2 and $\delta^{13}CO_2$ of pore fluids and simple two-component mixing of three possible ΣCO_2-sources: Dissolution of biogenic calcium carbonate which does not significantly affect the $\delta^{13}CO_2$; decomposition of sedimentary organic carbon (POC) which adds "light" ΣCO_2 of between −20‰ and −22‰ PDB; anaerobic oxidation of methane which generates extremely light ΣCO_2 depending whether the methane is thermogenic (−35‰ PDB) or biogenic (−65‰ PDB). Note: Stations 8408-04 (▲) and 8306-26(+) show ^{13}C-depletions as expected from POC decomposition; more strongly $^{13}CO_2$-depleted samples are from stations affected by fluid venting [8708-02 (■), 8306-24 (×), and 8306-27 (●)]; Station 8306-17 (○) [not discussed in this paper] from the abyssal plain bordering the Oregon overthrust to the north also shows very "light" ΣCO_2, probably derived from methane oxidation; *SW*=seawater.

sand layer at the bottom of Core 8306-26, with elevated contents of diagenetic carbonates (Han and Suess, this issue), shows some evidence for methane-derived CO_2. In this interval the predicted and measured ΣCO_2 deviate significantly from each other. We are uncertain of the reason for this discrepancy, but have observed the same phenomenon repeatedly within coarse-grained sediments in other parts of the Oregon-Washington subduction zone. Second, Cores 8306-27 and 8306-24 contain up to 30% methane-derived metabolic ΣCO_2, with significant proportions predicted all the way to the sediment-water interface. Third, cores 8708-03, 8708-02 and 8408-10 contain significant amounts of methane-derived ΣCO_2 only in pore fluids of the deeper core sections. These are overlain by sediments which contain no methane-derived ΣCO_2 but perhaps show evidence for aerobic methane oxidation. The overlying sediment cover varies in thickness.

In summary, then, we hypothesize — based on pore fluid chemical anomalies — that the sediments at the toe of the continental slope up to and including the scarps undergo early diagenesis of normal sedimentary organic matter by sulfate reduction and the sediments covering the seaward face of the main underthrust ridge and the ponded basin at the ridge crest show evidence for methane-derived metabolic ΣCO_2.

This interpretation is supported by the anomalous ^{13}C-depletion in the dissolved ΣCO_2 of selected samples of pore fluids from Cores 8306-24, 8306-26, 8306-27, and 8708-02 of the underthrust ridge and 8408-04 from the toe of the continental slope (Fig.6; Table III). We consider it particularly significant that certain carbon isotope values of the dissolved ΣCO_2, between −23‰ and −34‰ PDB, are more negative than the minimum values of −22‰ measured for POC from this area (Hedges and Mann, 1979; Hedges and Van Green, 1982). The latter would be the lowest value that could reasonably be explained by addition of metabolic ΣCO_2 solely from sedimentary POC sources (Claypool and Kaplan, 1974; Reeburgh, 1982). This trend is exemplified by the stable carbon isotope composition of interstitial ΣCO_2 of cores 8408-04 and 8306-26 unaffected by methane oxidation. In fact, the two samples 8408-10/125-130 and /160-163 we used to calculate the isotopic composition of ΣCO_2 generated from POC. The values ranged from −19.1 to −21.4‰ PDB, based on these, an average of −20‰ was used in the isotope balance discussed later. It has been shown for many recent and ancient anoxic environments that the $\delta^{13}C$ distribution in such pore fluids is explainable by

a mixing process between buried oceanic ΣCO_2 ($\delta^{13}C = +0.5‰$) and metabolic ΣCO_2 generated from mineralization of POC ($\delta^{13}C = -20‰$ PDB) (McCorkle, 1987). In oxic and suboxic environments, where metabolic ΣCO_2 dissolves skeletal carbonates — an important benthic process causing the sedimentary lysocline — skeletal-derived ΣCO_2 also effects the total dissolved ΣCO_2 pool (Emerson and Bender, 1981; Emerson et al., 1982; McCorkle, 1987). As described above, sulfate reduction produces alkalinity, and thus does not drive $CaCO_3$ dissolution. In the unlikely case that skeletal $CaCO_3$ dissolution would contribute ΣCO_2 it is similar isotopically to the oceanic ΣCO_2 and therefore would not cause a negative carbon isotope shift. The shallow pore fluids of the Oregon subduction zone which show a strong negative $\delta^{13}C$-shift are a rare occurrence and, so far, seem to be unique to the marginal ridge sediments which are affected by fluid expulsion from depth. We suggest that these isotope signatures clearly reflect the mineralized CH_4-substrate just as their NH_4^+-deficiency reflects the lack of organic nitrogen during CH_4-oxidation.

Carbon isotope balance for ΣCO_2

By including CH_4-substrate mineralization, the ΣCO_2 in pore fluids of the marginal ridge and their peculiar carbon isotope composition can be modelled as a three-component mixing process. The sources are: oceanic ΣCO_2 from buried seawater bicarbonate, metabolic ΣCO_2 from POC-mineralization and from CH_4-mineralization. With most of the parameters known in this system, or at least reasonable assumptions possible, we consider in the following discussion a carbon isotope balance and solve for the $\delta^{13}C$ of the hypothetical CH_4-derived portion of ΣCO_2.

In the isotope balance the quantity of ΣCO_2 is that actually measured in the pore fluid and which is generated by mineralization of one or both of the organic substrates, plus the buried oceanic ΣCO_2, minus the quantity removed by carbonate mineral formation. The amount of methane-derived ΣCO_2 is a critical quantity for the isotope balance. It is calculated from the ammonium and dissolved sulfate relationship (as previously shown) and adjusted for the ΣCO_2-removal by mineral precipitation. This adjustment is necessary for all the ΣCO_2-sources because otherwise the different terms are weighted unevenly.

Isotope fractionation during lithification by carbonate minerals is not yet taken into account because, at most, only 1–2‰ of absolute change in the dissolved ΣCO_2 is expected at the ambient temperatures of the Oregon margin sites. This fractionation, though, is less than the overall significance of the isotope balance.

The conditions for isotope balance of the pore water ΣCO_2 are expressed as follows:

$$\delta^{13}CO_{2\,(meas)}[\Sigma CO_{2\,(meas)}] = \delta^{13}CO_{2\,(sw)}[c] + \delta^{13}CO_{2\,(POC)}[b] + \delta^{13}CO_{2\,(meth)} \times [a] \quad (5)$$

Hereby $[a]$, $[b]$ and $[c]$ are the estimated concentrations of the three ΣCO_2 sources as follows:

$[\Sigma CO_{2\,(meth)}]$ = methane-derived CO_2 [mM]
$\delta^{13}CO_{2\,(meth)} = \delta^{13}C$ of methane-derived CO_2 (‰PDB)
$[\Sigma CO_{2\,(POC)}]$ = POC-derived CO_2 [mM]
$\delta^{13}CO_{2\,(POC)} = \delta^{13}C$ of POC-derived CO_2, calculated from two samples of Core 8408-04 $= -20$ (‰ PDB)
$[\Sigma CO_{2\,(sw)}]$ = inorganic ΣCO_2 of buried sea water, assumed to be 2.6 [mM]
$\delta^{13}CO_{2\,(sw)} = \delta^{13}C$ of buried seawater ΣCO_2, assumed to be $+0.5$ (‰ PDB)

On the left-hand side of Eq.(5) the measured parameters are:

$[\Sigma CO_{2\,(meas)}]$ = dissolved ΣCO_2 [mM]
$\delta^{13}CO_{2\,(meas)} = \delta^{13}C$ of ΣCO_2 in pore water (‰ PDB)

Solving for the unknown parameter $\delta^{13}CO_{2\,(meth)}$, yields a most interesting sequence of $\delta^{13}C$ values for the ΣCO_2 from mineralization of the postulated CH_4-substrate in cores 8306-24, 8306-27, and 8708-02 (Table IV). First,

TABLE IV

Predicted $\delta^{13}CO_2$ of methane-derived ΣCO_2 based on pore water isotope balance and calculated amount of methane-derived ΣCO_2. The three stations, 8306-24, 8306-27, and 8708-02 are affected by venting of methane-charged fluids. The uncertainty for the predicted $\delta^{13}C$ of the ΣCO_2 is based on a propagation of analytical errors of the pore water data (Table II)

Depth (cm)	$\Sigma CO_{2(meas)}$ (mM)	$\delta^{13}CO_{2(meas)}$ (‰ PDB)	Methane-derived $\delta^{13}CO_{2(pred)}$ (‰ PDB)
Core 8306-24			
25–30	0.61	−15.2	−37±4
85–90	2.09	−23.1	−59±6
160–165	4.42	−26.3	−51±5
Core 8306-27			
20–25	0.51	−13.3	−34±4
50–55	0.91	−19.2	−50±5
70–75	1.10	−20.7	−54±5
90–95	1.52	−21.3	−49±5
105–110	1.57	−23.4	−60±6
130–135	2.01	−24.3	−59±6
145–150	2.10	−24.7	−63±6
Core 8708-02			
60–70	0.20 (1.11)*	−13.5	−34±4
115–120	0.49 (1.09)	−23.9	−50±5
215–220	6.43	−34.8	−57±6

( )*: from discrepancy between predicted and measured ΣCO_2 assumed to be methane-derived by aerobic oxidation; see also Fig.4a.

the overall range of −35‰ to −63‰ PDB appears very reasonable for oxidation products of methane (Whiticar et al., 1986). Second, the systematic decrease in $\delta^{13}C$ with core depth, best shown by Core 8306-27, indicates a "reservoir effect" which follows the classical Rayleigh fractionation (Claypool and Kaplan, 1974). These findings encourage a more detailed discussion of the substrate sources and pool size.

Discussion: source of methane-derived ΣCO_2

At first glance the isotope signature of the postulated methane-driven ΣCO_2 (−35‰ and −63‰) indicates neither a biologic nor a thermal origin. Typical isotope values for biogenic methane are around −70 to −90‰ PDB and thermogenic methane is "heavier" by about 40–50‰ (Reeburgh, 1982; Whiticar et al., 1986). In case of thermogenic methane, the isotope fractionation during CH_4-oxidation would — if significant — require the CH_4-pool to be around −20‰ to 40‰ (Whiticar and Faber, 1986). Metabolic ΣCO_2 of biogenic methane can attain the predicted range of carbon isotopes only during oxidation in a closed system as the substrate pool diminishes considerably in size (Rayleigh effect; Claypool and Kaplan, 1974).

With only scarce data on methane contents and isotope signatures available from the Oregon subduction zone (Table V) we will discuss the model predictions in conjunction with other data which we have obtained from elsewhere (Whiticar et al., 1985, 1988). The data are from the Bransfield Strait basin of the Antarctic continental margin a back-arc basin environment of organic-rich sediments where, fortunate for this comparison, the center of the basin is dominated by biogenic methane production and consumption. The basin sediments are unaffected by tectonically-induced pore fluid flow (Suess et al., 1987b). At this site we have measured the systematic changes in stable carbon isotope composition of products and substrates as a large biogenic methane pool is progressively metabolized by microbial sulfate reducers. At Site 1327-1 in the Bransfield Strait, the biogenic methane (produced below the zone of dissolved sulfate exhaustion and with a $\delta^{13}C$ signature of < -100‰ PDB; Table V) diminishes as the gas diffuses upward into the sulfate reduction zone. During this passage the amount of methane strongly decreases and the residual gas becomes isotopically "heavier", i.e. it changes from −99 to −47‰ PDB, as the "lighter" fraction is preferentially metabolized. As a consequence, the product of this reaction — the accumulated ΣCO_2 — is significantly depleted in ^{13}C. Although the amount of methane-derived ΣCO_2 is small relative to the overwhelming contribution from mineralization of POC in the Bransfield Strait sediments, its isotope signa-

TABLE V

Comparison of a biogenic methane pool undergoing oxidation in the sulfate reduction zone of hemipelagic sediments of the Bransfield Strait and vent gasses and fluids in sediments of the Oregon subduction zone. The similarities in total gas content of the sediment, of around 100 ppb, and the isotope shift towards "lighter" ΣCO_2 supports our hypothesis that the vent fluids of the Oregon subduction zone contain biogenic methane. The isotope shift in D/H of the water also tends to support extensive methane oxidation for the Bransfield Strait environment but is inconclusive for the Oregon subduction zone

Depth (cm)	CH_4 (ppb)	C_2H_6 (ppb)	$\delta^{13}CH_4$ (‰ PDB)	ΣCO_2 (mM)	$\delta^{13}CO_2$ (‰ PDB)	SO_4^{2+} (mM)	$\delta D_{(water)}$ (‰ SMOW)
1327-1 Bransfield Strait, biogenic gas							
0–10	30[a]	2[a]	−47.3*	6.8	—	25.7	—
23–28	32	5	−51.4	11.8	−18.2	22.7	−8.0
49–53	39	1	−58.9	18.0	−19.8	20.5	−6.0
110–115	50	1	−60.3	29.1	−22.8	14.4	−2.7
200–205	82	1	−59.3	42.9	—	5.5	−9.4
sulfate reduction ends here methane formation begins							
320–325	7340	0	−99.7	53.3	−23.7	0.2	—
365–370	14890	0	−100.8	54.6	−20.9	0.4	−8.5
410–415	17470	0	−101.9	55.9	−21.6	0.2	−7.8
465–470	22540	0	−100.7	56	−20.4	0.1	−9.2
510–515	46380	0	−100.2	56	−14.9	0.1	−11.5
550–555	28740	0	−98.4	57	−14.0	<0.1	−10.8
630–635	16950	0	−94.9	56	−12.5	<0.1	−9.4
725–730	8560	0	−90.3	—	−10.5	—	−12.1
750–755	15480	0	−88.5	58	−7.2	0.6	−9.3
8708-02 Oregon margin, vent gas							
30–40	—	—	—	3.12	—	27.71	—
40–45	57	3.8	—	—	—	—	—
60–70	—	—	—	3.17	−13.5	27.17	—
92–98	—	—	—	3.27	—	27.28	—
98–103	75	4.5	—	—	—	—	—
115–120	—	—	—	3.29	−23.9	26.70	—
120–125	86	5.4	—	—	—	—	—
150–155	107	6.5	—	—	—	—	—
166–172	—	—	—	9.05	—	19.19	—
172–177	66	3.9	—	—	—	—	—
218–220	2	0.1	—	14.92	−34.8	11.36	—
sulfate reduction only							
8708-03 Oregon margin, vent gas							
20–26	—	—	—	3.56	—	26.59	—
26–31	80	4.5	—	—	—	—	—
56–61	—	—	—	4.13	—	24.44	—
62–67	73	4.6	—	—	—	—	—
112–117	—	—	—	9.88	—	18.93	—
118–121	91	5.2	—	—	—	—	—
sulfate reduction only							

[a]Data for shallowest sediment are from different station in Bransfield Strait; 1186-1 (Suess et al., 1987b).

ture is noticeable in the decreased ^{13}C-contents of around −23‰ PDB at the depths of maximum methane consumption between 205–325 cm. The magnitude of change in carbon isotope composition of the methane over the several meters of sulfate reduction zone in the Bransfield Strait is the same as that predicted by the isotope balance for the Oregon margin pore fluids. Even the range of absolute isotope values and the contents of the residual

methane in the Bransfield Strait basin sediments are identical to those in the Oregon subduction zone (Table V). For the scope of this discussion, it is therefore important to note that the hypothetical CH_4-type substrate from which the ΣCO_2 in the Oregon margin pore fluids derives is very likely biogenic. The gas must have originated from considerable depth and represent the last fraction — a few percent at most — of an original large biogenic methane pool. This is illustrated in Fig.7 which shows the changes in $\delta^{13}C$ predicted by the Rayleigh fractionation between the residual CH_4, the instantaneously produced ΣCO_2 and the cumulative ΣCO_4 pools. A kinetic fractionation factor, $\alpha = 1.014$, is used for the anaerobic oxidation reaction of methane (Whiticar and Faber, 1986) and an initial $\delta^{13}C$ for the methane of -67‰ PDB. This value was measured on free methane collected from the bottom waters of the Oregon margin vent site (Suess et al., 1987a). The trend shown by the cumulative ΣCO_2 pool would be the isotope composition if there were no removal of ΣCO_2 by carbonate mineral precipitation. Conversely, the trend shown by the instantaneously produced ΣCO_2 is that which would result if continuous carbonate mineral precipitation were to take place. The latter situation is the more realistic one judging from the ubiquitous presence of diagenetic carbonates around vents of the Oregon margin. Furthermore, the size of the remaining methane pool (between 4% and 28% of the initial pool) may be gleaned from Fig.7 by projecting the calculated range of CH_4-derived ΣCO_2 (Table IV) onto the trend given for the instantaneous ΣCO_2 production by the Rayleigh fractionation.

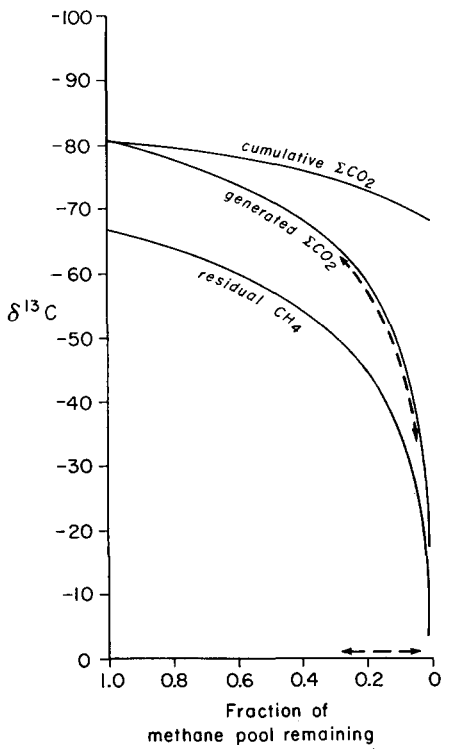

Fig.7. Carbon isotope distribution between methane and carbon dioxide pools during anaerobic methane oxidation as predicted by the Rayleigh fractionation process. $\delta^{13}C = -67$‰, measured on methane in bottom water of the Oregon vent site, was assumed for the initial reservoir (Suess et al., 1987b) along with a kinetic fractionation factor $\alpha = 1.014$ (Whiticar and Faber, 1986). The cumulative trend shows the change in $\delta^{13}C$ if all the metabolic ΣCO_2 remains in the system; the other trends show the $\delta^{13}C$ of the instantaneously generated ΣCO_2 and concurrent removal from the system such as by carbonate mineral precipitation and the $\delta^{13}C$ of the remaining methane pool, respectively. The range in $\delta^{13}C$ indicated by the broken line is that predicted for the pore water ΣCO_2 in Core 8306-27 (Table IV) which permits estimation of the site of the remaining CH_4-pool.

The deuterium/hydrogen ratios of the pore water could potentially also record the process of CH_4-oxidation because the H_2O) generated is highly depleted in deuterium; i.e. $\delta D = -224$‰ SMOW in methane (Whiticar et al., 1988). There is indeed a systematic change towards "lighter" δD-value in pore fluids from the Oregon underthrust ridge (Table III; 8306-24 and 8306-27). The scatter, however, in the data of the pore waters from the undeformed sediments (8408-10, and 8306-27) — which should have received no "light" water — is equally as large or larger than the δD-values of the underthrust ridge. A final interpretation, therefore, remains inconclusive. However, the data from the Bransfield Strait pore water (Table V; 1327-1) show a stronger enrichment in "light" water where we expect a larger amount of CH_4 being oxidized. In the methane generation zone below there is even "lighter" water, which is apparently contradictory un-

less it reflects higher accumulation of methane oxidation products with longer time or — as is plausible for this site — the input of glacial melt water. At present we do not fully understand all the sources for "light" water that could enter the pore water system in any of the sedimentary environments and conclude that CH_4-oxidation is indeed a potential process for the D/H-isotope shift observed — for which we present here qualitative data — but are unable to quantitatively demonstrate such a reaction.

Finally, there is interesting supportive evidence for a changing reservoir of oxidizable methane and the accompanying carbon isotope shift from the $\delta^{13}C$ distribution of a concentric dolomite nodule recovered from the Oregon vent site. The mineralogy, trace element and stable isotope characteristics of this nodule were originally described by Ritger et al. (1987). These authors interpreted the growth structure and progressively more negative $\delta^{13}C$ values from the center towards the rim of the nodule (i.e. from −39‰ to −34‰) as the result of a change in mixing ratio of seawater-derived "heavy" ΣCO_2 and methane-derived "light" ΣCO_2.

The authors also indicated that, alternatively, the trend may reflect a shift in the initial methane reservoir from "heavy" to "light" $\delta^{13}CH_4$ during carbonate mineral precipitation. We have documented in the preceeding sections such shifts in the measured down-core $\delta^{13}C$ of the pore water ΣCO_2 and the hypothetical methane substrate (Table IV; Core 8306-27). Therefore, we support the latter explanation and suggest, as an extension, that the nodule's center may have formed from the oxidation products of a more strongly ^{13}C-enriched biogenic methane reservoir (i.e., with more residual "heavy" methane) located close to the sediment-water interface and the subsequent layers formed when the nodule was located at greater depth in the core and in contact with a less ^{13}C-enriched methane reservoir (i.e. containing more "light" methane). At coring Site 8708-02, the same locality from which the nodule was recovered, the predicted $\Sigma^{13}CO_2$ pool indicates that the center of the nodule may have formed in an environment equivalent to that found at a depth of 60–70 cm. Here the metabolic ΣCO_2 ($\delta^{13}C = -34.8$‰) is derived from a ^{13}C-enriched methane pool. The nodule continued to grow with increased burial depth and the outer layers ($\delta^{13}C = -39$‰ PDB) precipitated from ΣCO_2 of a less ^{13}C-enriched methane pool, i.e. ~ -50‰ PDB at 115–120 cm below the seafloor. A reservoir of biogenic methane in the undeformed Astoria fan sediments is well-documented by the range of $\delta^{13}C$ of CH_4 from −78 to −88‰ PDB (Claypool, 1974).

Summary

We wished to document that anomalies in the stoichiometry of dissolved ammonium, sulfate, and ΣCO_2 of pore waters from those sediments which are affected by fluid venting in the Oregon subduction zone can be used to quantify the oxidation of a methane substrate by microbial sulfate reducers. Venting of methane-charged fluids is an important process of active continental margins undergoing lateral compression. On passive margins hydrocarbon seeps and submarine aquifers also discharge methane-rich fluids (Paull et al., 1984; Brooks et al., 1987; Hovland et al., 1987), although apparently less important in magnitude on a global scale than the plate convergence-induced fluid expulsion. The isotope composition of the metabolic carbon dioxide resulting from the oxidation of methane is recorded in the $\delta^{13}C$ of carbonate mineral cements, concretions, and chimneys which are frequently found at subduction vents. Qualitatively, the effect of methane oxidation seems also evident in a significant decrease in the δD signal in pore waters. The range of stable carbon isotope values, in turn, is controlled by the degree to which the methane substrate reservoir is oxidized. Changes in reservoir size can be related to burial depth only if venting and oxidation rates are constant. Generally, though, the dynamics of venting and oxidation rates determine the degree of consumption of the methane reservoir, the stable carbon iso-

tope composition of residual methane and the dissolved ΣCO_2 resulting from its oxidation, and the depth below seafloor of carbonate mineral formation. We envision that during high flow rates a less ^{13}C-enriched methane pool enters the zone of carbonate mineral formation from below producing isotopically "light" nodules (i.e. −60‰ PDB) and during slow venting, strongly ^{13}C-enriched methane reaches the reaction zone producing "heavier" nodules (i.e. −34‰ PDB). If no venting occurs at all, the biogenic methane reservoir — which forms in most hemipelagic sediments along continental margins — remains at depths of several hundreds of meters and does not reach the sulfate reduction zone where carbonate minerals form. In the case of convergence-induced venting — which very likely is a process of global significance along all subduction zones — the variations in chemistry and stable isotopes of diagenetic carbonates contain a great deal of information on the venting process.

Acknowledgements

Many colleagues have contributed through advice, criticism, and by asking the right questions at the right time to the development of our ideas presented here. We especially thank L. D. Kulm (OSU) for outstanding support in the task of placing the coring transect in the optimal tectonic framework of the Oregon convergent margin. Jacques Boulegue, Université P. et M. Curie was a most gracious host and supporter of subduction-induced venting as evidenced from pore fluid chemical anomalies. Numerous discussions with him advanced our thinking on this subject; he also presented and defended this paper, in our absence, at the Kaiko Conference in 1986. Many thanks to Dan McCorkle for a most helpful review of an earlier version of this manuscript.

The crew and masters of the research vessels *Wecoma* and *Atlantis II* provided expert support in critical coring operations during three cruises in 1983, 1984, and 1987. We are indebted to M. von Breymann, C. A. Ungerer, P. Kalk, and A. Harrison, S. Pullen (OSU) and U. Moeller and A. Tallig (BGR) for their valuable assistance during ship-board and subsequent shore-based analytical work.

This study is part of the senior author's ongoing project with L. D. Kulm, co-principal investigator, on the "Fluid Venting Process in the Oregon Accretionary Complex" which is funded by the National Science Foundation grants OCE-8215147 and OCE-8609789. Additional financial support was provided by Centre National Recherche Scientifique of France and the Oregon State University Foundation.

References

Berner, R. A., 1977. Stoichiometric models for nutrient generation in anoxic sediments. Limnol. Oceanogr., 22: 781–786.

Berner, R. A., 1980. Early Diagenesis: A Theoretical Approach. Princeton Univ. Press, Princeton, N.J., 237 pp.

Boatman, C.D. and Murray, J.W., 1982. Modeling exchangeable NH_4^+-adsorption in marine sediments: Process and controls of adsorption. Limnol. Oceanogr., 27: 99–110.

Boulegue, J., Iiyama, J. T., Charlou, J. L. and Jedwab, J., 1987. Nankai Trough, Japan Trench and Kuril Trench: Geochemistry of fluids sampled by submersible "*Nautile*". Earth Planet Sci. Lett., 83: 363–375.

Bremner, J. M., 1960. Determination of nitrogen in soil by the Kjeldahl method. J. Agric. Sci., 55: 11–33.

Brooks, J. M., Kennicutt II, M. C., Fischer, C. R., Macko, S. A., Cole, K., Childress, J. J., Bidigare, R. R. and Vetter, R. D., 1987. Deep-Sea hydro-carbon seep communities: Evidence for energy and nutritional carbon sources. Sciences, 238: 1138–1142.

Childress, J. J., Fisher, T. J., Brooks, J. M., Kennicutt II, J. M., Bidigare, R. R. and Anderson, A., 1986. A methanotropic marine molluscan (Bivalvia Mytilidae) Symbiosis: Mussels fueled by gas. Science, 233: 1306–1308.

Claypool, G. E., 1974. Anoxic Diagenesis and Bacterial Methane Production in Deep Sea Sediments. Ph.D. Thesis, Univ. Calif. Los Angeles, Calif., 276 pp.

Claypool, G. E. and Kaplan, I. R., 1974. The origin and distribution of methane in marine sediments. In: I. R. Kaplan (Editor), Natural Gases in Marine Sediments. Plenum, New York, N.Y., pp. 99–139.

Coleman, M. L., Shepherd, Th. J., Durham, J. J., Rouse, J. E. and Moore, G. R., 1982. Reduction of water with zinc for hydrogen isotope analysis. Anal. Chem., 54: 993–995.

Devol, A. H., 1983. Methane oxidation rates in the anaerobic sediments of Saanich Inlet. Limnol. Oceanogr., 28: 738–742.

Emerson, S. and Bender, M., 1981. Carbon fluxes at the

sediment water interface of the deep sea: calcium carbonate preservation. J. Mar. Res., 39(1): 139–162.

Emerson, S., Grundmanis, V. and Graham, D.W., 1982. Carbonate chemistry in marine pore waters: MANOP sites C and S. Earth Planet. Sci. Lett., 61: 220–232.

Grasshoff, K., 1976. Methods of Seawater Analysis. Verlag Chemie, Weinheim-New York, N.Y., 317 pp.

Han, M. W., 1987. Dynamics and Chemistry of Pore Fluids in Marine Sediments of Different Tectonic Settings: Oregon Subduction Zone and Bransfield Strait Extensional Basin. Ph.D. Thesis, Oregon State Univ., Corvallis, OR, 280 pp.

Han, M. W. and Suess, E., 1989. Subduction-induced pore fluid venting and the formation of authigenic carbonates along the Cascadia continental margin: Implications for the global Ca-cycle. Palaeogeogr., Palaeoclimatol., Palaeoecol., 71: 97–118.

Hartmann, M., Müller, P. J., Suess, E. and van der Weijden, C.H., 1973. Chemistry of late Quaternary sediments and their interstitial waters from the NW-African continental margin. "Meteor" Forsch.-Ergebn., C-24: 1–67.

Hedges, J. I. and Mann, D. C., 1979. The lignin geochemistry of marine sediments from the southern Washington coast. Geochim. Cosmochim. Acta, 43: 1809–1818.

Hedges, J. I. and Van Green, A., 1982. A comparison of lignin and stable carbon isotope compositions in Quaternary marine sediments. Mar. Chem., 11: 43–54.

Hovland, M., Talbot, M. R., Qvale, M. R., Olaussen, S. and Aasberg, L., 1987. Methane-related carbonate cements in pockmarks of the North Sea. J. Sediment. Petrol., 57: 881–892.

Iversen, N. and Jørgensen, B. B., 1985. Anaerobic methane oxidation rates at the sulfate-methane transition in marine sediments from Kattegat and Skagerrak (Denmark). Limnol. Oceanogr., 30: 944–955.

Kulm, L. D. and Fowler, G. A., 1974. Oregon continental margin structure and stratigraphy: a test of the imbricate thrust model. In: C. A. Burk and C. L. Drake (Editors), The Geology of Continental Margins. Springer, New York, N.Y., pp. 261–283.

Kulm, L. D., Suess, E., Moore, J. C., Carson, B., Lewis, B. T., Ritger, S. D., Kadko, D. C., Thornburg, T. M., Embley, R. W., Rugh, W. D., Massoth, G. J., Langseth, M. G., Cochrane, G. R. and Scamman, R. L., 1986. Oregon subduction zone: venting, fauna, and carbonates. Science, 231: 561–566.

LePichon, X., Iiyama, T., Boulegue, J., Charvet, J., Faure, M., Kano, K., Lallemant, S., Okada, H., Rangin, C., Taira, A., Urabe, T. and Uyeda, S., 1987. Nankai Trough and Zenisu Ridge: a deep-sea submersible survey. Earth Planet. Sci. Lett., 83: 285–299.

Manheim, F. T. and Sayles, F. L., 1974. Composition and origin of interstitial waters of marine sediments based on deep sea drill cores. In: E. D. Goldberg (Editor), The Sea. Wiley, New York, N.Y., 5: 527–568.

McCorkle, D. C., 1987. Stable carbon Isotopes in Deep Sea Pore Waters: Modern Geochemistry and Paleoceanographic Applications. Ph.D. Dissertation, Univ. of Washington, Seattle, Wash., 209 pp.

Moore, J. C., Mascle, A., Taylor, E., Andrieff, P., Alvarez, F., Barnes, R., Beck, C., Behrmann, J., Blanc, G., Brown, K., Clark, M., Dolan, J., Fisher, A., Gieskes, J. and others, 1986. Structural and hydrologic framework of the northern Barbados ridge: results of Leg 110 ODP. International Kaiko Conference on subduction zones, 10–15 November, Tokyo and Shimizu, p. 25.

Paull, C. K., Hecker, B., Commeau, R., Freeman-Lynde, R. P., Neuman, C., Corso, W. P., Golubic, S., Hook, J. E., Sikes, E. and Curray, J., 1984. Biological communities at the Florida Escarpment resemble hydrothermal vent taxa. Science, 226: 965–967.

Reeburgh, W. S., 1982. A major sink and flux control for marine sediments: Anaerobic consumption. In: K. A. Fannig and F. T. Manheim (Editors), The Dynamic Environment of the Ocean Floor. Lexington Books, Lexington and Toronto, pp. 203–217.

Ritger, S., Carson, B. and Suess, E., 1987. "Methane-derived authigenic carbonates formed by subduction-induced pore water expulsion along the Oregon/Washington margin". Geol. Soc. Am. Bull., 98: 147–156.

Rosenfeld, J. K., 1981. Nitrogen diagenesis in Long Island Sound sediments. Am. J. Sci., 281: 436–462.

Russell, K. L., Deffeyes, K. S. and Fowler, G. A., 1967. Marine dolomite of unusual isotopic composition. Science, 155: 189–191.

Scamman, R. L., 1981. Diagenetic Carbonate Cementation of Clastic Sediments near the Sediment-Water Interface on the lower Continental Slope off Washington and northern Oregon. Thesis, Lehigh Univ., Bethlehem, Pa., 197 pp.

Schroeder, N. A. M., Kulm, L. D. and Muehlberg, G. E., 1987. Carbonate chimneys on the outer continental shelf: evidence for fluid venting on the Oregon margin. Oreg. Geol., 49(8): 91–96.

Silva, J. A. and Bremner, J. M., 1966. Determination and isotope-ratio analysis of different forms of nitrogen in soils: 5. Fixed ammonium. Soil Sci. Soc. Am. Proc., 30: 587–594.

Suess, E., 1976. Nutrients near the depositional interface. In: I. N. McCave (Editor), The Benthic Boundary Layer. Plenum Press, New York, N.Y., pp. 57–77.

Suess, E., Carson, B., Ritger, S. D., Moore, J. C., Jones, M. L., Kulm, L. D. and Cochrane, G. R., 1985. Biological communities at vent sites along the subduction zone off Oregon. In: M. L. Jones (Editor), The Hydrothermal Vents of the Eastern Pacific: An Overview. Bull. Biol. Soc. Wash., 6: 475–484.

Suess, E., Kulm, L. D., Carson, B. and Whiticar, M. J., 1987a. Fluid flow and methane fluxes from vent sites at the Oregon subduction zone. EOS, 68(44): 1486.

Suess, E., Fisk, M. and Kadko, D., 1987b. Thermal interaction between back-arc volcanism and basin sediments in the Bransfield Strait, Antarctica. Antarc. J. U.S., 22(5): 47–49.

Von Breymann, M., 1987. Magnesium in Hemipelagic Environments: Surface Reactions in the Sediment-Pore Water System. Ph.D. Dissertation, Oregon State University, Corvallis, OR, 216 pp.

Watermann, L. S., Sayles, F. L. and Manheim, F. T., 1972.

Interstitial water studies on small core samples Leg 16, 17, and 18. In: Initial Reports of the Deep Sea Drilling Project, Vol. 18. U.S. Govt. Printing Office, Washington, D.C., pp. 1001–1012.

Weliky, K., Suess, E., Ungerer, C. A., Müller, P. J. and Fischer, K., 1983. Problems with accurate carbon measurements in marine sediments and particulate matter in seawater: A new approach. Limnol. Oceanogr., 28: 1252–1259.

Whiticar, M. J. and Faber, E., 1986. Methane oxidation in marine and limnic sediments and water columns. 12th Intl. Mtg. Organic Geochemistry 1985, Juelich. In: D. Leythaeuser and J. Rullkötter (Editors), Advances in Organic Geochemistry, Vol. 10, Springer, New York, N.Y., pp. 759–768.

Whiticar, M. J., Suess, E. and Wehner, H., 1985. Thermogenic hydrocarbons in surface sediments of the Bransfield Strait, Antarctica. Nature, 314: 87–90.

Whiticar, M. J., Faber, E. and Schoell, M., 1986. Biogenic methane formation in marine and freshwater environments: CO_2 reduction vs. acetate fermentation: Isotope evidence. Geochim. Cosmochim. Acta, 50(5): 693–709.

Whiticar, M. J., Suess, E. and Wefer, G., 1988. Calcium carbonate hexahydrate (ikaite): History of mineral formation as recorded by stable isotopes. Earth Planet. Sci. Lett. (submitted).